The University of Sydney

School of Civil Engineering
Sydney NSW 2006
AUSTRALIA

http://www.civil.usyd.edu.au/

Centre for Advanced Structural Engineering

Distortional Buckling of Overhanging Monorails

Research Report No R906

N S Trahair BSc BE MEngSc PhD DEng

October 2009

The University of Sydney

School of Civil Engineering
Centre for Advanced Structural Engineering
http://www.civil.usyd.edu.au/

Distortional Buckling of Overhanging Monorails

Research Report No R906

N S Trahair BSc BE MEngSc PhD DEng

October 2009

Abstract:

This paper is concerned with the elastic lateral-distortional (LD) buckling of overhanging steel monorail I-beams and its influence on their design strengths. Distortion of a slender web reduces the elastic buckling resistance of an intermediate length beam below its flexural-torsional (FT) resistance.

A finite element computer program was used to study the elastic LD buckling of overhanging monorails with bottom flange loads at the free ends. The ratio M_{LD} / M_{FT} of the elastic LD to FT buckling moments decreased significantly as the flange width-thickness ratio b_f/t_f decreased, but varied only slightly with the web depth-thickness ratio b_w/t_w. The value of M_{LD} varied almost linearly with the ratio of the supported span to the overhang length, and the effect of top flange torsional restraint at the exterior support on M_{LD} was similar to that on M_{FT}. Distortion effects were very small when there was no torsional restraint, but increased significantly with the torsional restraint stiffness. The full plastic moment was often reached before M_{LD}, especially for low values of b_f/t_f and high values of the torsion parameter K.

Conservative approximations were developed for predicting the elastic LD buckling moments for ranges of sections, slendernesses, span ratios, and torsional restraint stiffnesses.

A method of designing overhanging steel monorails against LD buckling was proposed and its use demonstrated by a worked example.

Keywords: beams, bending, buckling, design, distortion, elasticity, member resistance, monorails, overhanging, steel, torsion.

Copyright Notice

Distortional Buckling of Overhanging Monorails

N.Trahair@civil.usyd.edu.au

Published by:
School of Civil Engineering
The University of Sydney
Sydney NSW 2006
AUSTRALIA

October 2009

http://www.civil.usyd.edu.au

1. Introduction

It is difficult to design steel I-section beams used as overhanging monorails (Fig. 1) because they are not well restrained against lateral deflection, twisting, and distortion, so that they are likely to buckle laterally. The free end of the overhanging monorail is only restrained against distortion by web stiffeners which provide an end stop for the load trolley. At the exterior support, the top flange is prevented from deflecting laterally, but the compression bottom flange is not directly restrained. Because there is no web stiffener here to prevent distortion of the cross-section, any restraint provided to the compression flange by a top flange torsional restraint is decreased by distortion of the web.

Design codes [1-4] generally provide methods of designing beams against flexural-torsional (FT) buckling (Fig. 2b), but these ignore any distortion of the cross-section. These methods might be applied to overhanging monorails by compensating partially for distortion by omitting the effects of top flange torsional restraints, but the results are likely to be of uncertain accuracy, and may be over-conservative. If advantage is to be taken of the strengthening effects of torsional restraints, then the effects of distortion need to be accounted for by replacing the FT buckling analysis [5] by a lateral-torsional (LD) buckling analysis (Fig. 2c) [6-10].

The purposes of this paper are to investigate the elastic LD buckling of the overhanging monorail shown in Fig. 1, and to develop a method of design against LD buckling. There are so many variables that it is necessary to limit the problems studied for this paper. It is assumed that end stops prevent distortion of the end cross-sections, that the load acts at the free end at the bottom flange, and that the monorail is uniform and of doubly symmetric I-section. Ranges of section dimensions, member lengths, and degrees of top flange torsional restraint at the exterior support are considered. The effects of distortion on elastic buckling are expressed as reduction factors by which the elastic FT buckling loads must be multiplied.

2. Previous research

Tanner [11] developed an approximate method for designing overhanging monorails against FT buckling. His method ignored the strengthening effects of the warping rigidity of the section and the application of the load to the bottom flange instead of at the shear centre. No allowance was made for the weakening effects of distortion, and crude approximations were made for the effective length and the effect of the moment distribution.

Trahair [12] developed a method for designing a wide range of single span, two span, cantilevered and overhanging monorails against FT buckling. This accounted for the warping rigidity, the application of the load to the bottom flange, and the effects of the moment distribution. The effects of distortion were ignored, but these were compensated for by an unknown extent by ignoring the effects of torsional restraints acting on the top flange at the supports.

While there have been many studies of the LD buckling of beams, some of which are summarized in [8] and [10], a significant development was made in [6, 7], which developed a computer program based on the finite strip method of analyzing the elastic buckling of simply supported thin-walled open section beam-columns in uniform compression and bending. A simple approximate method of analyzing the LD buckling of simply supported I-section members in uniform compression and bending was developed in [8], and extended in [9] to members with more general restraint and loading conditions.

Bradford [13] analysed the elastic LD buckling of overhanging beams whose exterior support was connected to the bottom flange, and showed that distortion caused significant reductions in the elastic buckling resistance, especially when the load at the free end acted at the top flange. This study is not directly relevant to a monorails with a bottom flange load and whose exterior support is connected to the top flange.

Ozdemir and Topkaya [14] analysed the elastic LD buckling of single overhanging monorails with free end bottom flange loads by using shell elements in a commercial computer program. The monorails had no web stiffeners at their free ends and a range of partial depth web stiffeners at the exterior top flange support, where twist rotations were generally assumed to be prevented. The values of the flange width b_f, flange thickness t_f, web thickness t_w and overall length $L(1+\gamma)$ were generally fixed, but the web depth b_w varied. The predicted elastic buckling moments were presented as fractions of the uniform bending FT buckling moment of a simply supported beam of the overall length of the monorail. Partial depth web stiffeners at the exterior supports were found to be almost as effective as full depth stiffeners. The LD buckling moments of double overhanging monorails with partial depth web stiffeners and whose top flange rotations were prevented at the supports were found to be very close to those of single overhanging monorails.

Trahair [15] extended the research on the FT buckling of single span monorails [12] to include the effects of distortion and of torsional restraints at the supports. The beams considered had wide ranges of section dimensions and beam lengths. It was found that the strength reductions caused by distortion were small because distortion at the supports was prevented by the monorail end stops. However, the results are not directly relevant to overhanging monorails.

3. Elastic flexural-torsional buckling

3.1. Top flange free to twist at the exterior support

A monorail with a supported span and a single overhang is shown in Fig. 1. The supported span is prevented from deflecting (u = 0) and twisting (ϕ = 0) at the interior support and its top flange is prevented from deflecting (u_T = 0) but is free to twist ($\phi_T \neq 0$) at the exterior support. The monorail load acts at the bottom flange at the free end. The variations of the dimensionless elastic FT buckling moment M_{FT0} have been analysed using the computer program PRFELB [16, 17]. These may be approximated [12] by using

$$\frac{M_{FT0}L}{\sqrt{EI_y GJ}} = \{1 \quad \gamma \quad \gamma^2\}[c_0]\{1 \quad K \quad K^2\}^T \tag{1}$$

and

$$[c_0] = \begin{bmatrix} 2.32 & 1.96 & 0.262 \\ -1.26 & -1.18 & -0.209 \\ 0.252 & 0.248 & 0.0421 \end{bmatrix} \tag{2}$$

in which E (= 200,000 MPa) and G (= 76923 MPa) are the Young's and shear moduli of elasticity, I_y and J are the minor axis second moment of area and torsion section constant, L is the overhang length, γ is the ratio of the supported span length to the overhang length, and K is the torsion parameter

$$K = \sqrt{\frac{\pi^2 EI_w}{GJL^2}} \tag{3}$$

in which I_w is the warping section constant.

3.2. Top flange prevented from twisting at the exterior support

When the top flange of the monorail has a rigid torsional restraint (ϕ_T = 0) at the exterior support, the variations of the dimensionless elastic FT buckling moment $M_{FT\infty}$ with the length ratio γ and the torsion parameter K may be approximated by using

$$\frac{M_{FT\infty}L}{\sqrt{EI_y GJ}} = \{1 \quad \gamma \quad \gamma^2\}[c_\infty]\{1 \quad K \quad K^2\}^T \tag{4}$$

and

$$[c_\infty] = \begin{bmatrix} 2.94 & 9.69 & 0.383 \\ 2.20 & -9.29 & 0.149 \\ -1.14 & 2.38 & -0.125 \end{bmatrix} \tag{5}$$

The effects of the span ratio γ and the torsion parameter K on the dimensionless elastic FT buckling moment $M_{FT\infty} L/\sqrt{(EI_yGJ)}$ of some of the sections shown in Table 1 are shown in Fig. 3.

3.3. Top flange with elastic torsional restraint at the exterior support

When the top flange of the monorail has an elastic torsional restraint of stiffness α_{rz} at the exterior support, the variations of the dimensionless elastic FT buckling moment may be approximated by using the values of M_{FT} obtained from

$$\frac{(M_{FT} - M_{FT0})}{(M_{FT\infty} - M_{FT0})} = \frac{\alpha_{rz}^*}{(\beta + \alpha_{rz}^*)} \tag{6}$$

in which

$$\alpha_{rz}^* = \frac{\alpha_{rz} L}{GJ} \tag{7}$$

$$\beta = \{1 \quad \gamma \quad \gamma^2\}[d]\{1 \quad K \quad K^2\}^T \tag{8}$$

and

$$[d] = \begin{bmatrix} 8.18 & 0.929 & 11.6 \\ -4.27 & -0.260 & -10.3 \\ 0.751 & -0.168 & 2.56 \end{bmatrix} \tag{9}$$

The effects of top flange torsional restraint on the dimensionless elastic FT buckling moments $M_{FT} L/\sqrt{(EI_yGJ)}$ for a span ratio of $\gamma = 2.0$ are shown in Fig. 4.

4. Elastic lateral-distortional buckling

4.1. Buckling analysis

A finite element method of analyzing the elastic LD buckling of uniform I-section beams under general loading and restraint conditions was developed in [9]. The nodal deformations consist of the top (T) and bottom (B) flange lateral displacements u and twist rotations ϕ shown in Fig. 2c and lateral rotations u' ($\equiv \mathrm{d}u/\mathrm{d}z$). This method uses cubic deformation approximations for the variations of u and ϕ with the distance z along each element and a cubic approximation for the web displacements down the web. If there is a rigid web stiffener (RWS) which prevents local web distortion at a point along the beam, then some of the deformations at that point are related through

$$\begin{aligned} \phi_T - (u_T - u_B)/b_w &= 0 \\ \phi_B - (u_T - u_B)/b_w &= 0 \end{aligned} \tag{10}$$

This method was used in [15] to study the effects of top flange torsional restraints at the supports of single span monorails.

The cross-sections considered were chosen so that the web b_w / t_w did not exceed 75 (design codes [1-4] usually apply severe restrictions to unstiffened webs with higher values) and the flange $b_f / 2t_f$ did not exceed 16 (again, design codes usually apply severe restrictions to flanges with higher values). Details of the nine different cross-sections considered are shown in Table 1. These have values of b_f / t_f = 128 / 16, 204.8 / 10, and 256 / 8 (designated by FL, FM, FH in Table 1, in which L, M, H indicate, low, medium and high slenderness), and b_w / t_w = 200 / 6, 240 / 5, and 300 / 4 (designated by WL, WM, WH in Table 1).

The same sections have been used for this paper to analyse the effects of distortion on the elastic buckling of the overhanging monorail shown in Fig. 1. The overhanging monorail has a bottom flange concentrated load acting at the free end, where web stiffeners prevent distortion (RWS). The top flange is prevented from deflecting laterally and elastically restrained against twisting at the exterior support. Both flanges are prevented from deflecting laterally at the interior support where web stiffeners prevent distortion. The results are presented in Figs 3 – 6.

4.2. Top flange prevented from twisting at the exterior support

The variations of the dimensionless elastic LD buckling moments $M_{LD\infty} L/\sqrt{(EI_yGJ)}$ with the torsion parameter $K = \sqrt{(\pi^2 EI_w / GJL^2)}$ are compared with the dimensionless elastic FT buckling moments $M_{FT\infty} L/\sqrt{(EI_yGJ)}$ for overhanging monorails with rigid torsional top flange restraints at the exterior support (α_{rz} = ∞) in Fig. 5 for 3 different sections and a span length ratio of γ = 2.0. The effects of distortion are very significant for rigid torsional restraint, especially for monorails of low flange slenderness (FL) with high values of K (and low values of L).

Also shown in Fig. 5 are the variations of the dimensionless full plastic moments $M_p L/\sqrt{(EI_yGJ)}$ with the torsion parameter K for monorails with yield stress f_y = 300 MPa. These indicate that the full plastic moments will often be reached before elastic LD buckling occurs, especially for monorails of low flange slenderness (FL) with high values of K.

The effects of the span ratio γ on elastic LD buckling are demonstrated in Fig. 3, where it can be seen that the dimensionless elastic LD buckling moment $M_{LD\infty} L/\sqrt{(EI_yGJ)}$ varies almost linearly with the span ratio γ.

The variations of the ratio M_{LD}/M_{FT} of the elastic LD and FT buckling moments (which provides a correction factor for estimating the effect of distortion on the elastic buckling resistance) with the slenderness $\sqrt{(M_L/M_{FT})}$, in which M_L is the elastic local buckling (Fig. 2a) moment are shown in Fig. 6 for the case of a span length ratio of γ = 2.0. This form of slenderness was chosen because both the LD buckling reductions below M_{FT} and the local buckling moments M_L are significantly affected by the effective web slenderness which is influenced by any restraining effects of the compression flange. Thus $\sqrt{(M_L/M_{FT})}$ can be thought of as a measure of the effective web slenderness. Approximate values of M_L may be obtained from [15], while accurate values for the sections considered are given in Table 1.

The variations shown in Fig. 6 for monorails with γ = 2.0 indicate that the ratio M_{LD}/M_{FT} decreases from 1 towards M_L/M_{FT} as the slenderness $\sqrt{(M_L/M_{FT})}$ decreases. The rate of decrease varies little with the web slenderness b_w/t_w but increases significantly as the flange slenderness b_f/t_f decreases (the same indications were found in [15] for single span simply supported monorails). This is because the resistance of a beam with low slenderness flanges depends mainly on the flexural stiffness of the compression flange in restraining lateral deflection. This stiffness is proportional to b_f^3/t_f, which is comparatively small for a low slenderness flange. On the other hand, the resistance of a beam with high slenderness flanges depends more on the combined flexural and torsional stiffnesses of the compression flange in restraining both lateral deflection and twist rotation. This combined stiffness is proportional to b_f^2/t_f^2.

In some cases, the value of M_{LD}/M_{FT} exceeds that of M_L/M_{FT}, probably because the (low) length L is such that the true local buckling moment (under moment gradient) is higher than the minimum value used for M_L (based on uniform bending). It may be noted that the values of code section slenderness limits are conservative compared with those derived from M_L, since the code limits ignore the strengthening effects of local buckling interactions between the flanges and web, and allow for the effects of yielding and imperfections.

4.3. Top flange free to twist at the exterior support

The variations of the dimensionless elastic LD buckling moments $M_{LD0}L/\sqrt{(EI_yGJ)}$ with the torsion parameter K are compared with the dimensionless elastic FT buckling moments $M_{FT0}L/\sqrt{(EI_yGJ)}$ for overhanging monorails without top flange restraints at the exterior support (α_{rz} = 0) in Fig. 5 for 3 different sections and a span length ratio of γ = 2.0. The effects of distortion are very small.

4.4. Top flange with elastic torsional restraint at the exterior support

The effects of top flange elastic torsional restraint on the dimensionless elastic LD buckling moment $M_{LD}\,L/\sqrt{(EI_yGJ)}$ for a span ratio of α = 2.0 are shown in Fig. 4. It can be concluded that $M_{LD}\,L/\sqrt{(EI_yGJ)}$ may be conservatively approximated by using a linear approximation of the same type as that of Equation 6 used to approximate the effects of top flange elastic torsional restraints on the dimensionless elastic FT buckling moment $M_{FT}\,L/\sqrt{(EI_yGJ)}$.

4.5. Approximations

Designers need a relatively simple but safe method of predicting the effects of distortion on the buckling of overhanging monorails. Such a method can be developed by noting the findings illustrated in Figs 3 – 6. Fig. 3 shows that the effect of torsional restraint at the top flange at the exterior support can be predicted conservatively by assuming that the elastic buckling moment varies linearly with the restraint stiffness parameter α_{rz}*/(β+α_{rz}*). Fig. 4 shows that the effect of the span ratio γ can be predicted conservatively by assuming that the elastic buckling moment varies linearly with γ. Thus an approximate value of the elastic buckling moment M_{LD} can be determined by using

$$\begin{aligned} M_{LD} = &\left(\frac{\beta}{\beta+\alpha_{rz}^*}\right)\{(M_{LD10}(2-\gamma)+M_{LD20}(\gamma-1)\} \\ &+\left(\frac{\alpha_{rz}^*}{\beta+\alpha_{rz}^*}\right)\{(M_{LD1\infty}(2-\gamma)+M_{LD2\infty}(\gamma-1)\} \end{aligned} \tag{11}$$

in which M_{LD10}, M_{LD20} are the values of M_{LD} for γ = 1, 2 and α_{rz} = 0, and $M_{LD1\infty}$, $M_{LD2\infty}$ are the corresponding values for α_{rz} = ∞.

Fig. 5 shows that the effect of distortion is small when α_{rz} = 0, in which case M_{LD10}, M_{LD20} may be approximated by using

$$M_{LD10} = M_{FT10}(1-0.054K) \tag{12a}$$

$$M_{LD20} = M_{FT20}(1-0.034K) \tag{12b}$$

in which M_{FT10}, M_{FT20} are the values of the elastic FT buckling moments obtained from Equations 1 and 2 for γ = 1, 2.

Fig. 6 shows that $M_{LD\infty}$ / $M_{FT\infty}$ (in which $M_{FT\infty}$ is the value of the elastic FT buckling moment obtained from Equations 4 and 5) decreases from 1 at high slendernesses $\sqrt{(M_L / M_{FT\infty})}$ to $M_L / M_{FT\infty}$ at low slendernesses. Conservative estimates of the value of $M_{LD\infty}$ / $M_{FT\infty}$ can be obtained by using the value of

$$\frac{M_{LD\infty}}{M_{FT\infty}} = \left(\frac{1 + k_d + M_L / M_{FT\infty}}{2} \right) - \sqrt{\left(\frac{1 + k_d + M_L / M_{FT\infty}}{2} \right)^2 - \frac{M_L}{M_{FT\infty}}} \quad (13)$$

in which k_d is a factor which allows for the effects of distortion for the particular cross-section. A family of curves defined by this approximation is shown in Fig. 7.

Values of k_d obtained by matching the curves of Fig. 7 with those of Fig. 6 for monorails with γ = 2 are given in Table 2. These values are closely approximated by

$$k_{d2} = \begin{Bmatrix} 1 \\ 0.1 b_w / t_w \\ (0.1 b_w / t_w)^2 \end{Bmatrix}^T \begin{bmatrix} 4.18 & 0.333 & -0.0528 \\ -3.87 & 0.0779 & 0.00857 \\ 0.79 & -0.0521 & 0.00239 \end{bmatrix} \begin{Bmatrix} 1 \\ 0.1 b_f / t_f \\ (0.1 b_f / t_f)^2 \end{Bmatrix} \quad (14)$$

Values of k_d obtained for monorails with γ = 1 are also given in Table 2. These values are closely approximated by

$$k_{d1} = \begin{Bmatrix} 1 \\ 0.1 b_w / t_w \\ (0.1 b_w / t_w)^2 \end{Bmatrix}^T \begin{bmatrix} 3.341 & -2.46 & 0.451 \\ 1.427 & -1.261 & 0.2503 \\ -0.1928 & 0.1821 & -0.03745 \end{bmatrix} \begin{Bmatrix} 1 \\ 0.1 b_f / t_f \\ (0.1 b_f / t_f)^2 \end{Bmatrix} \quad (15)$$

5. Design against lateral-distortional buckling

Although design codes generally [1-4] have rules for designing beams against FT buckling, very few have rules which allow the economical design of monorails which are loaded at or below the bottom flange. The Australian code AS4100 [1] and the European code EC3 [3] have a general method of design by buckling analysis [18, 19] which allows the direct use of the result of an elastic FT buckling analysis such as those performed for this paper. For this, the elastic buckling moment M_{FT} is used in the equation

$$\frac{M_b}{M_p} = \frac{1}{\Phi + \sqrt{(\Phi^2 - M_p / M_{FT})}} \le 1 \quad (16)$$

in which

$$\Phi = 0.5\{1 - 0.49[\sqrt{(M_p / M_{FT})} - 0.2] + M_p / M_{FT}\} \quad (17)$$

for compact welded beams with b_w/b_f < 2 to determine the nominal major axis moment resistance M_b.

Code rules for design against FT buckling are sometimes used for design against LD buckling. It is consistent with these uses to apply the method of design by buckling analysis to LD buckling by modifying Equations 16 and 17 by replacing M_{FT} by the elastic LD buckling moment M_{LD}.

6. Worked example

6.1. Problem

Determine the nominal design moment resistance M_b of a welded overhanging monorail whose section properties are those of Section FL/WL in Table 1. The overhanging length is L = 3.2 m, the supported span length is γL = 4.8 m, the yield stress is f_y = 300 MPa, and the stiffness of the top flange torsional restraint at the exterior support is α_{rz} = 2E7 Nmm/rad.

6.2. Flexural-torsional buckling

Using Equation 3, K = 0.621
Using Equations 1 and 2 and γ=1.0, M_{FT10} = 10.98 kNm.
Using Equations 1 and 2 and γ=2.0, M_{FT20} = 6.526 kNm.
Using Equations 4 and 5 and γ=1.0, $M_{FT1\infty}$ = 32.53 kNm.
Using Equations 4 and 5 and γ=2.0, $M_{FT2\infty}$ = 17.92 kNm.
Using Equation 7, α_{rz}* = 2.286
Using Equations 8 and 9, β = 4.300
Using Equation 6, M_{FT} = 139.5 kNm.

6.3. Lateral-distortional buckling

Using Equation 12a, M_{LD10} = 106.2 kNm.
Using Equation 12b, M_{LD20} = 63.88 kNm.
Using Equation 15, k_{d1} = 2.800
Using Equation 14, k_{d2} = 2.303
Using Equation 13, $M_{LD1\infty}$ = 229.5 kNm.
Using Equation 13, $M_{LD2\infty}$ = 151.5 kNm.
Using Equation 11, M_{LD} = 121.6 kNm.

6.4. Design

Using Equation 17, Φ_{FT} = 1.202
Using Equation 16, M_{bFT} = 75.67 kNm.
Using Equation 17, Φ_{LD} = 1.294
Using Equation 16, M_{bLD}= 70.02 kNm.

7. Conclusions

This paper is concerned with the elastic lateral-distortional (LD) buckling of overhanging steel monorail I-beams and its influence on their design strengths. The bottom compression flange of the monorail is unrestrained at the free end and only partially restrained at the exterior support, and so is likely to buckle laterally at low loads. While torsional top flange restraint at the exterior support will increase the buckling resistance, this will be reduced by web distortion effects. The elastic LD buckling loads provide a transition from the elastic local (L) buckling loads of short length beams to the elastic FT buckling loads of long length beams.

A finite element computer program was used to study the effects of cross-section, slenderness, span ratio, and torsional restraint on the elastic LD buckling of overhanging monorails with bottom flange loads at the free ends. The effects of web distortion were expressed by the variations of the ratio M_{LD} / M_{FT} of the elastic LD to FT buckling moments with the slenderness $\sqrt{(M_L/M_{FT})}$ determined using the elastic local buckling moment M_L. This ratio decreased significantly as the flange width-thickness ratio b_f/t_f decreased, but varied only slightly with the web depth-thickness ratio b_w/t_w. The value of M_{LD} varied almost linearly with the span ratio γ, and the effect of the torsional restraint stiffness α_{rz} on M_{LD} was similar to that on the flexural-torsional buckling moment M_{FT}. Distortion effects were very small when there was no torsional restraint, but increased significantly with the torsional restraint stiffness. The full plastic moment M_p was often reached before M_{LD}, especially for low values of b_f/t_f and high values of the torsion parameter K.

Conservative approximations were developed for predicting the elastic LD buckling moment for ranges of sections, slendernesses, span ratios, and torsional restraint stiffnesses.

The method of design by buckling analysis used or implied in some codes for design against FT buckling was adapted for designing steel overhanging monorails against lateral-distortional buckling. A worked example was given with a summary of its solution.

References

[1] SA. AS 4100-1998 Steel structures. Sydney: Standards Australia; 1998.

[2] BSI. BS5950 Structural use of steelwork in building. Part 1:2000. Code of practice for design in simple and continuous construction: Hot rolled sections. London: British Standards Institution; 2000.

[3] BSI. Eurocode 3: Design of steel structures: Part 1.1 General rules and rules for buildings, BS EN 1993-1-1. London: British Standards Institution; 2005.

[4] AISC. Specification for structural steel buildings. Chicago: American Institute of Steel Construction; 2005.

[5] Trahair NS. Flexural-torsional buckling of structures. London: E & FN Spon; 1993.

[6] Hancock GJ. Local, distortional, and lateral buckling of I-beams. Journal of the Structural Division ASCE, 1978; 104 (ST11): 1787-98.

[7] Papangelis JP, Hancock, GJ. THIN-WALL – Cross-section analysis and finite strip buckling analysis of thin-walled structures. Centre for Advanced Structural Engineering University of Sydney; 1997.

[8] Hancock GJ, Bradford MA, Trahair NS. Web distortion and flexural-torsional buckling. Journal of the Structural Division ASCE, 1980; 106 (ST7): 1557-71.

[9] Bradford MA, Trahair NS. Distortional buckling of I-beams. Journal of the Structural Division ASCE, 1981; 107 (ST2): 355-70.

[10] Bradford MA. Lateral-distortional buckling of steel I-section members. Journal of Constructional Steel Research, 1992; 23: 97-116.

[11] Tanner NS. Allowable bending stresses for overhanging monorails. AISC Engineering Journal, 1985; (3): 133-8.

[12] Trahair NS. Lateral buckling of monorail beams. Engineering Structures, 2008; 30: 3213-8.

[13] Bradford MA. Elastic distortional buckling of overhanging beams. Structural Engineering and Mechanics, 1996; 4 (1): 37-47.

[14] Ozdemir KM, Topkaya C. Lateral buckling of overhanging crane trolley monorails. Engineering Structures, 2006; 28 (8): 1162-72.

[15] Trahair NS. Lateral-distortional buckling of monorails. Engineering Structures, 2009; doi: 10.1016/j.engstruct.2009.07.013.

[16] Papangelis JP, Trahair NS, Hancock GJ. PRFELB – Finite element flexural-torsional buckling analysis of plane frames. Centre for Advanced Structural Engineering, University of Sydney; 1997.

[17] Papangelis JP, Trahair NS, Hancock GJ. Elastic flexural-torsional buckling of structures by computer. Computers and Structures 1998; 68: 125 - 37.

[18] Trahair, NS, Bradford, MA, Nethercot, DA, Gardner, L. The Behaviour and Design of Steel Structures to EC3. London: Taylor and Francis; 2008.

[19] Trahair NS. Buckling analysis design of steel frames. Journal of Constructional Steel Research, 2009; 65(7):1459-63.

Notation

b_f, b_w	flange width and web depth
B,T	bottom and top flange
$c_{0,\infty}$	see Equations 2 and 5
d	see Equation 9
E	Young's modulus of elasticity
FT	flexural-torsional
F, W	flange and web
f_y	yield stress
G	shear modulus of elasticity
I_y	second moment of area about the y principal axis
I_w	warping section constant
J	torsion section constant
K	$= \sqrt{(\pi^2 EI_w/GJL^2)}$
k_d	distortion factor
L	length
L	local
LD	lateral-distortional
L, M, H	low, medium, and high slenderness
M	bending moment
M_b	nominal moment resistance
M_{FT}	maximum moment at elastic FT buckling
M_L	moment at elastic local buckling
M_{LD}	maximum moment at elastic LD buckling
M_p	fully plastic moment about the x axis
Q	end load
RWS	degree of freedom associated with a rigid web stiffener
t_f, t_w	flange and web thicknesses
u	lateral deflection
x, y	principal axes
α_{rz}	stiffness of top flange torsional restraint
α_{rz}*	$= \alpha_{rz} L/GJ$
β	see Equations 8 and 9
γ	span ratio
ϕ	twist rotation
0,∞	$\alpha_{rz} = 0, \infty$
1,2	$\gamma = 1, 2$

Table 1. Section Details

Quantity	b_f/t_f	b_w/t_w	I_y	J	I_w	M_L	M_p
Units	(mm/mm)	(mm/mm)	(mm^4)	(mm^4)	(mm^6)	(kNm)	(kNm)
FL/WH	128/16	300/4	5.592E6	353.9E3	125.8E9	869.6	211.3
FL/WM	128/16	240/5	5.592E6	359.5E3	80.53E9	1687	169.1
FL/WL	128/16	200/6	5.592E6	363.9E3	55.92E9	2411	140.9
FM/WH	204.8/10	300/4	14.32E6	142.9E3	322.1E9	567.5	211.3
FM/WM	204.8/10	240/5	14.32E6	146.5E3	206.2E9	501.8	169.1
FM/WL	204.8/10	200/6	14.32E6	150.9E3	143.2E9	458.8	140.9
FH/WH	256/8	300/4	22.37E6	93.78E3	503.3E9	256.9	211.3
FH/WM	256/8	240/5	22.37E6	97.38E3	322.1E9	232.8	169.1
FH/WL	256/8	200/6	22.37E6	101.8E3	223.7E9	218.5	140.9

Table 2. Values of k_d for $\alpha_{rz} = \infty$, $\gamma = 2.0, 1.0$

	FL - 128/16	FM - 204.8/10	FH - 256/8
WH - 300/4	1.8, 2.0	0.20, 0.70	0.20, 0.11
WM - 240/5	2.3, 2.8	0.30, 0.22	0.10, 0.02
WL - 200/6	2.3, 2.8	0.20, 0.10	0.04, 0.01

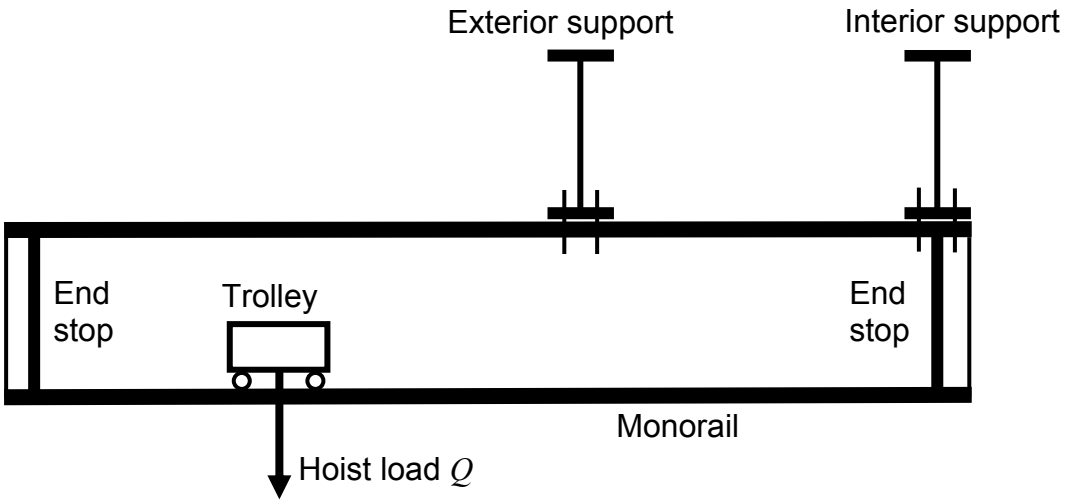

Fig. 1 Overhanging Monorail

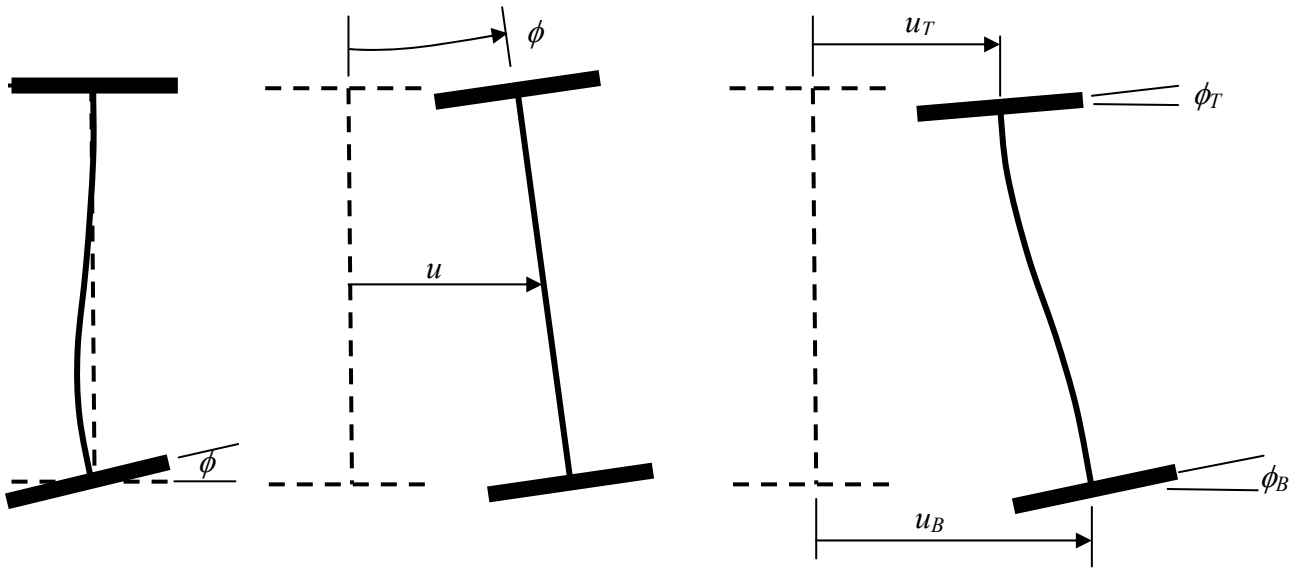

(a) Local buckling (b) Flexural-torsional buckling (c) Lateral-distortional buckling

Fig. 2. Buckling Modes

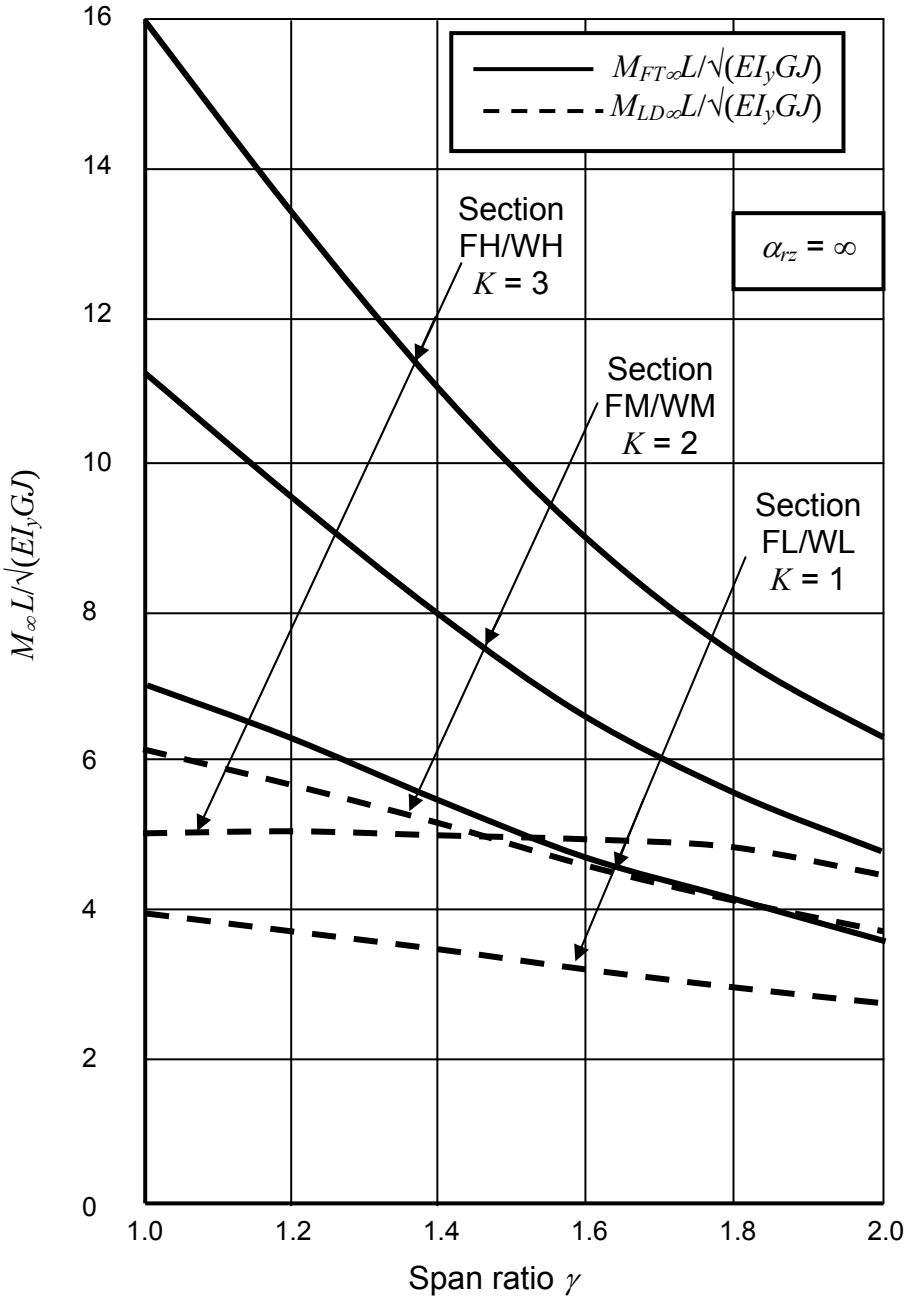

Fig. 3 Effect of Span Ratio γ

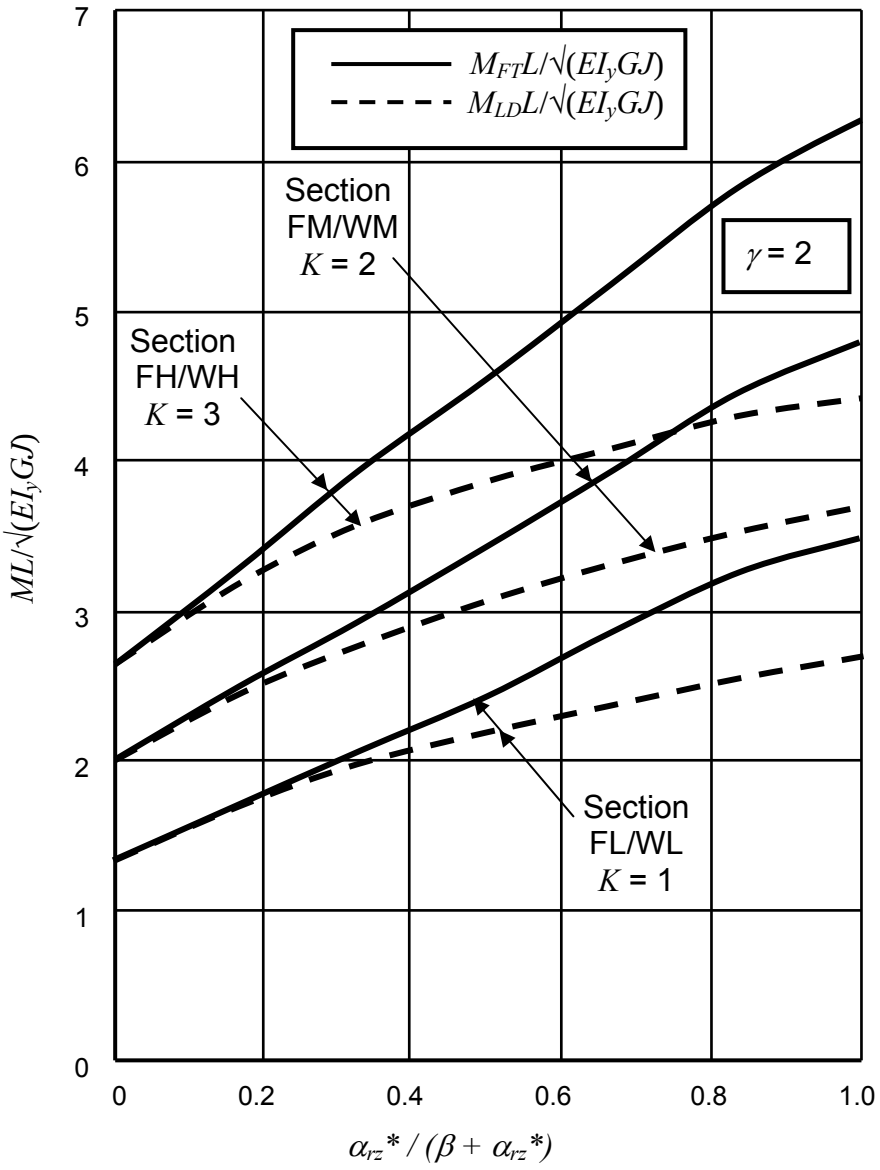

Fig. 4 Effect of Elastic Torsional Restraint

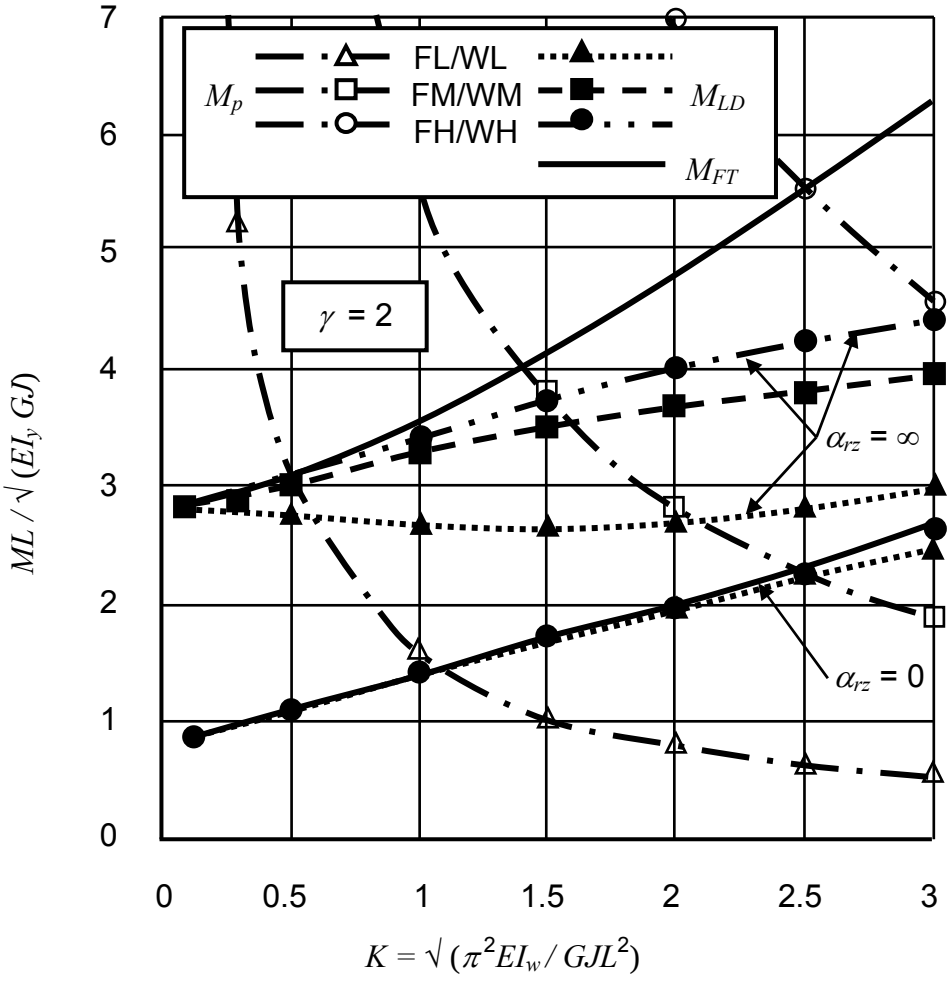

Fig. 5 Dimensionless LD Buckling Moments

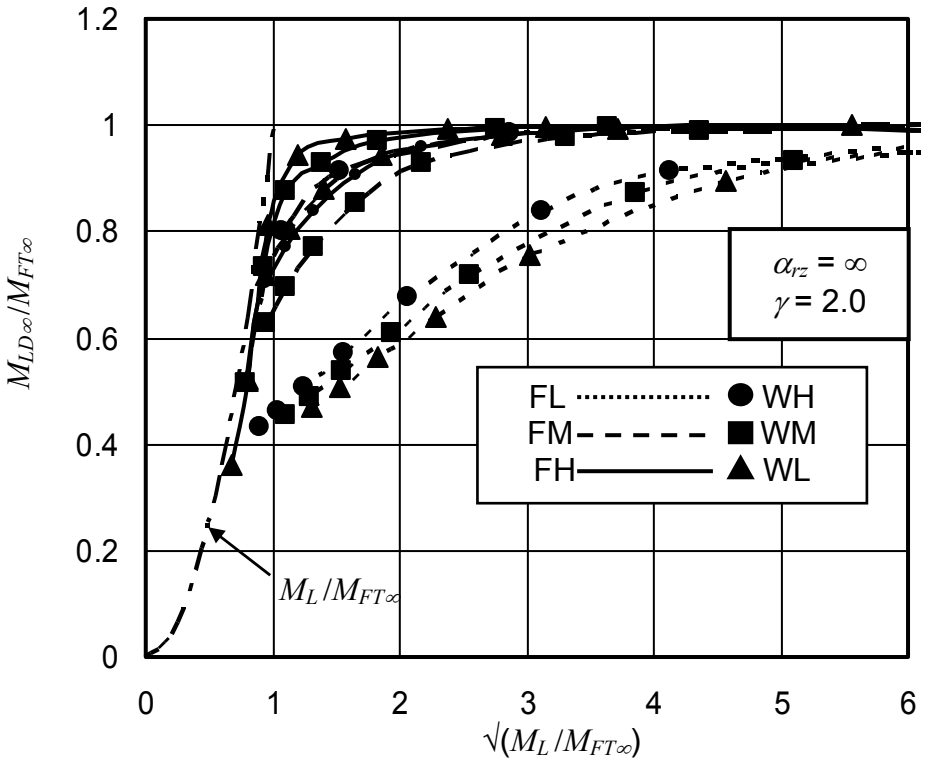

Fig. 6 Effects of Distortion

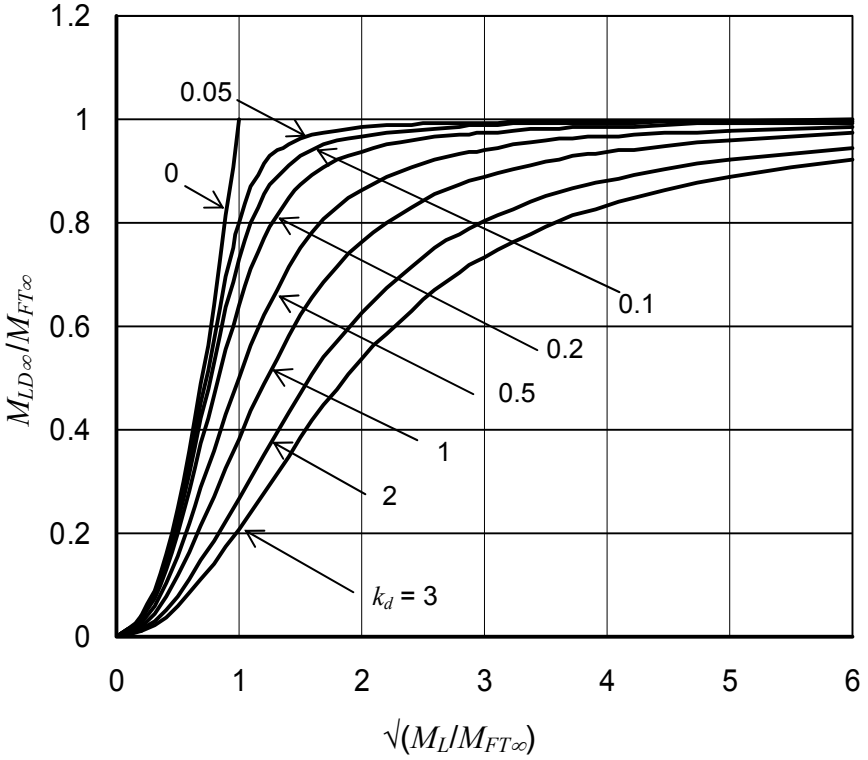

Fig. 7 Approximating Curves for $M_{LD}/M_{FT\infty}$